THE ANATOMICAL RECORD 246:47–63 (1996)

Evidence of Structural and Material Adaptation to Specific Strain Features in Cortical Bone

J.G. SKEDROS, M.W. MASON, M.C. NELSON, AND R.D. BLOEBAUM

Bone and Joint Research Laboratories, V.A. Medical Center, and Division of Orthopedic Surgery, University of Utah School of Medicine, Salt Lake City, Utah (J.G.S., M.C.N., R.D.B.); Musculoskeletal Research Laboratories, Department of Orthopaedics and Rehabilitation, Pennsylvania State University College of Medicine, Hershey, Pennsylvania (M.W.M.)

ABSTRACT ***Background:*** **Functionally induced strains provide epigenetic signaling for bone modeling and remodeling activities. Strain gauge documentation of the equine third metacarpal reveals a neutral axis passing through the craniolateral cortex, resulting in a narrow band of cortex loaded predominantly in tension, with the remainder of the cortex experiencing a wide range of compression strain magnitudes that are maximal in the caudomedial cortex. This predictable strain pattern provides a model for examining the hypothesis that strain mode, magnitude, and strain energy density are potential correlates of compact bone structural and material organization.**

Methods: **Structural and material variables were quantified in nine equine (standard breeds) third metacarpals for comparison with the in vivo strain milieu that was evaluated in thoroughbred horses. The variables quantified included secondary osteon population density (OPD), fractional area of secondary bone (FASB), fractional area of porous spaces, collagen fiber orientation, mineral content (% ash), and cortical thickness. Each bone was sectioned transversely at 50% of length, with subsequent quantification of eight radial sectors and three intracortical regions (periosteal, middle, endosteal). Linear regression analysis compared these variables to magnitudes of corresponding regional in vivo longitudinal strain, shear strain, and strain energy density values reported in the literature.**

Results: **The craniolateral ("tension") cortex of this bone is distinguished by its 30% lower FASB and with the lateral cortex exhibits 20% darker gray level (more longitudinal collagen) compared with the average of all other locations. Conversely, the remaining ("compression") cortices as a group have a high OPD, are more extensively remodeled, and contain more oblique-to-transverse collagen. The caudal cortices (caudomedial, caudal, caudolateral) are significantly thinner ($P < 0.01$) and have 4% lower mineral content ($P < 0.05$) than all other locations. Moderately strong correlations exist between collagen fiber orientation and normal strain ($r = 0.752$) and shear strain ($r = 0.555$). When normal and shear strains were transformed to their respective absolute values, thus eliminating the effects of strain mode (tension vs. compression), these correlation coefficients decreased markedly.**

Conclusions: **Collagen fiber orientation is related to strain mode and may function to accentuate rather than attenuate bending. These differences may represent adaptations that function synergistically with bone geometry to promote a beneficial strain distribution and loading predictability during functional loading.** © 1996 Wiley-Liss, Inc.

Key words: Bone strain, Bone adaptation, Collagen fiber orientation, Horse metacarpal, Osteons

Various mechanical features produced when a limb bone is functionally loaded have been proposed as preeminent or contributory stimuli in activating or inhibiting the modeling and remodeling processes that

Received April 5, 1995; accepted March 22, 1996.

Address reprint requests to R.D. Bloebaum, Ph.D., Bone and Joint Research Laboratories, V.A. Medical Center (151F), 500 Foothill Blvd., Salt Lake City, UT 84148.

achieve and subsequently maintain mechanically relevant adaptations in cortical bone. These include stress (Lanyon and Bourn, 1979; Martin and Burr, 1989), the strain tensor (Cowin, 1987), and various specific strain-related features including mode (or "polarity"; e.g., tension, compression, and shear), magnitude, rate, strain energy density, and frequency (Burr, 1992; Martin and Burr; 1989; Brown et al., 1990; Turner et al., 1995).

Skedros et al. (1994a,b) suggested that mechanically relevant regional adaptations to specific strain features, if present in steady-state remodeling of skeletal maturity, would be most clearly manifest in bones, where a long history of repetitive unidirectional bending predominates. They hypothesized that this may be related to the markedly different mechanical properties of bone in compression vs. tension. Their work on the mule deer calcaneus, a simple cantilevered bending system, shows what appear to be strain-mode-related mineral content and microstructural differences between tension and compression cortical locations. Similar large mineral content differences have also been reported in elk and horse calcanei (Skedros et al., 1993a). They cautioned, however, that the firmly adherent plantar ligament in these bones may affect the adjacent tension cortex through stress shielding or through the association of other non–strain-related stimuli. Noting that the magnitudes of compression strains are invariably greater than the magnitudes of tension strains, they were reticent to conclude that the differences reported were wholly related to strain mode.

Mason et al. (1995) and Riggs et al. (1993a,b) studied the structural and material organization of the equine radius, which is an eccentrically loaded long bone that experiences tension in its cranial cortex and compression in its caudal cortex. In contrast with the artiodactyl calcaneus, the equine radius lacks a firmly adherent, unicortical fibrous tension member. Regional differences in the amount of remodeled cortex and preferred collagen fiber orientation between opposite cortices in this bone may also be adaptations related to prevailing tension and compression strains. By using a broad age range of standard-breed horse radii, Riggs et al. (1993a) showed that the more extensive remodeling in the compression cortex serves to adjust regional elastic moduli by reorienting the longitudinal collagen seen in the radius of younger animals (foals) to the more oblique-to-transverse collagen seen in skeletal maturity. However, using the equine radius in an attempt to establish a link between specific strain features and potential adaptive enhancement, or accommodation, of a specific strain milieu is, like the deer calcaneus, confounded by the fact that the compression cortex experiences strains of greater magnitude than seen in the tension cortex (Turner et al., 1975; Schneider et al., 1982; Rubin and Lanyon, 1982; Biewener et al., 1983b). Furthermore, because the intracortical strain environment is inferred from surface strain data, correlation of the matrix organization in specific intracortical regions with strain magnitude variations must be suspect. Therefore, it is difficult to differentiate adaptations that might be associated with strain mode from those that might be associated with normal strain magnitudes or with other strain features.

The equine third metacarpal is a model which overcomes some limitations of the calcaneus and radius models. In vivo strain gauge studies of this bone are comparatively abundant (Biewener et al., 1983a,b; Davies et al., 1993; Gray and Rubin, 1988; Gross et al., 1990, 1991; Nunamaker et al., 1990; Turner et al., 1975). Gross et al. (1991, 1992) created a finite element model of the functionally loaded equine third metacarpal by using in vivo strain data collected from three rosette strain gauges placed equidistantly around the cortex at the same transverse location. The finite element model gives a more detailed description of intracortical strain variation at the mid-diaphysis of this bone at various gaits and speeds. Although the equine third metacarpal was previously considered to be loaded purely in compression (Biewener et al., 1983a,b), this bone is now known to have a neutral axis passing through the outer portion of the craniolateral cortex (Gross et al., 1992). During controlled gaits, this spatially consistent bending results in a narrow band of craniolateral cortex loaded in tension, with the remainder of the cortex experiencing a wide spectrum of compression strain magnitudes. The intracortical location of the neutral axis (during controlled gaits) facilitates the examination of cortical locations receiving tension and compression strains of similar magnitude for evidence of corresponding strain-mode-related differences in tissue organization.

Whether the cells responsible for attainment and maintenance of normal bone morphology perceive or respond to strain signals directly or indirectly is not yet clear. In either case experimental evidence suggests that this information is mediated through the bone matrix during functional loading (Burr, 1992; Lanyon, 1993; Brand and Stanford, 1994; Mullender and Huiskes, 1995). Therefore, detailed knowledge of the interplay between strain environment and matrix organization is needed to advance understanding of the matrix-mediated regulation of these cellular functions. The objective of the present study is to extend and clarify previous work on how various structural and material features may be used to deduce how a bone's morphology promotes or accommodates a long history of specific strain features produced during functional loading. We hypothesize that evidence of adaptive remodeling is related to a history of strain modes and that bone remodeling correlates with the spatial distribution of this strain feature. To test this hypothesis, the equine third metacarpal is examined for correlations between its in vivo strain milieu and its microstructure, collagen fiber orientation, mineral content, and cortical thickness.

METHODS

One third metacarpal bone was obtained from each of 10 skeletally mature standard-breed horses with no evidence of skeletal pathology at the time of death. The animals were selected from a larger sample of animals that had been taken to a regional abattoir over a period of 1 year. The range of animal weights was estimated to be 400–450 kg, and, hence, these animals were within 15% of the body weight of typical thoroughbreds. Skeletal maturity was confirmed by gross and roentgenographic examinations showing complete coosification of the epiphyseal growth plates of the radius, third metacarpal, and calcaneus. Among these

bones, the growth plate at the distal end of the radius is the last to fuse, and this occurs between approximately 2 to 3.5 years of age. In contrast, the third metacarpal fuses between approximately 1.7 and 18 months (Fretz et al., 1984).

Each bone was manually cleaned of soft tissues and sectioned transversely at 50% of its length. Two 5-mm-thick segments were subsequently cut proximal and distal to this initial transection. All sectioning was accomplished by using a variable-speed, water-cooled diamond blade band saw with a 0.3-mm kerf loss (Exact Instruments, Germany). The proximal segments were used for mineral content analysis and cortical thickness measurements and the distal segments for microstructure and collagen fiber orientation analysis, as described below.

Microstructure

The 5-mm-thick segments cut distal to 50% of bone length were embedded in polymethyl methacrylate (PMMA) by using conventional techniques (Emmanual et al., 1987). Each segment was then ground, polished, and prepared for backscattered electron (BSE) imaging in the scanning electron microscope (Skedros et al., 1993b; Bloebaum et al., 1990). Orientation lines were etched on the polished surface of each embedded specimen to define eight radial sectors: cranial, craniolateral, lateral, caudolateral, caudal, caudomedial, medial, and craniomedial (Fig. 1). With each sector, three regions representing three cortical "depths" were imaged: periosteal, middle, and endosteal. (Previously, we used the following terms to describe these three regions: pericortical, middle, and endocortical; Skedros et al., 1994b; Mason et al., 1995.) One ×50 high-resolution BSE image (1.6 × 2.3 mm) was taken in each region and recorded on Polaroid 52 film. The image in the periosteal region was immediately adjacent to the periosteal surface. The image in the middle region was equidistant between those taken in the periosteal and endosteal regions, and in the endosteal region was adjacent to the endosteal surface without including trabecular bone (Skedros et al., 1994b).

A sector was defined to have uniform width between periosteal and endosteal surfaces (Fig. 1). The width of the sectors approximates the width of two mesh points in the finite element model of Gross et al. (1992). Approximately 25% of the total area of each region was sampled by one BSE image. The conclusion that the area of one BSE image would adequately sample a cortical region was based prospectively on the suggested guidelines of Kimmel and Jee (1983), which were also employed in our past studies (Skedros et al., 1994b; Mason et al., 1995).

The BSE images were analyzed for the following variables by using standard stereologic point-counting techniques (Parfitt, 1983; Russ, 1986; Skedros et al., 1994b): secondary osteon population density (OPD), fractional area of secondary bone (FASB), and fractional area of porosity (porosity).

Secondary osteons, in contrast with primary osteons, were identified by using conventional microscopic criteria employed by Skedros et al. (1994b) and others (Corondan and Haworth, 1986; Barth et al., 1992). The following were counted as secondary osteons: (1) complete secondary osteons, (2) partially formed osteons in which the entire circumference of the preceding resorption space was lined with new bone; and (3) osteon fragments that had a complete central canal. Osteon population density was defined as the number of secondary osteons/mm^2 of bone.

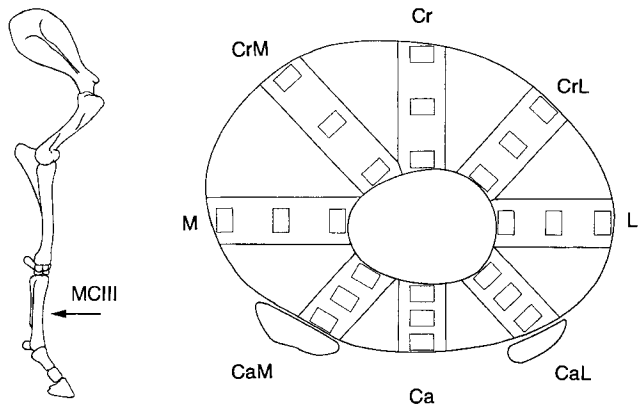

Fig. 1. **Left:** The drawing shows a lateral-to-medial view of the equine right forelimb skeleton. The arrow indicates the location of sectioning. **Right:** The drawing is a schematic representation of the third metacarpal (MCIII) cross section. Rectangles represent the locations of the images in the three regions (periosteal, middle, endosteal) at each of the eight radial sectors. In each region, microstructure, collagen fiber orientation, and mineral content were quantified. The splint bones (metacarpals II and IV) are also demonstrated. Cr, cranial; Crl, craniolateral; L, lateral; CaL, caudolateral; Ca, caudal; CaM, caudomedial; M, medial; CrM, craniomedial. (Copyright, J.G. Skedros, all rights reserved)

The FASB was determined by using a 9.5-mm grid randomly superimposed over each BSE image, resulting in 101 ± 4 sampling points. Each point was classified as either secondary or nonsecondary bone. Nonsecondary bone included primary osteon, plexiform, and interstitial bone (Skedros et al., 1994b). To maintain consistent terminology with past studies (Skedros et al., 1994a,b; Mason et al., 1995), the fractional area of secondary bone is expressed as the percentage of total bone area occupied by secondary osteon bone: (secondary bone area/total bone area) × 100.

Porosity measurements were made by using a 3.5-mm grid, representing 862 ± 10 sampling points, that was randomly superimposed over each BSE image. Those points falling in central canals of secondary osteons, central canals of primary osteons, resorption spaces, and Volkmann's canals were counted as porous spaces: (total porosity/total bone area) × 100. Our protocol required that images in the endosteal region be taken where bone area exceeded that of intervening porous spaces (Skedros et al., 1994b). Therefore, these data exclude the prominent porous transition zone observed qualitatively near the cortical and trabecular bone in some locations in these same specimens.

Mineral Content and Cortical Thickness

The 5-mm segments cut immediately proximal to the 50% level were meticulously cleaned of adherent soft tissues. Cortical thickness was measured to the nearest 0.01 mm at the eight cortical sectors by using a digital caliper (Mituyoyo, Japan). Measurements of the caudolateral and caudomedial cortices excluded the adherent splint bones (metacarpals II and IV). In all cases,

the splint bones formed a fibrous attachment at the 50% diaphyseal level. For the purposes of the present study, their exclusion is supported by data of Piotrowski et al. (1983), which shows that the splint bones exert a significant influence in bone geometric properties only in the proximal 30% of this bone.

With the water-cooled diamond-blade band saw, each of these segments were then cut into eight pieces, corresponding to the eight sectors imaged for microstructure quantification. By using a sharp osteotome, each piece was then cut into thirds, resulting in one specimen from each of the periosteal, middle, and endosteal regions. By using conventional methods described by Skedros et al. (1993c), the specimens were thoroughly defatted in full-strength chloroform for 20 days, dried to constant weight at 80°C, and ashed at 550°C for 24 hr. In accordance with terminology used in past studies, mineral content (% ash) of the bone matrix is expressed by dividing the weight of the ashed bone (W_{ab}) by the weight of the dried, defatted bone (W_{db}), and multiplying this number by 100 [(W_{ab}/W_{db}) × 100] (Currey, 1984; Skedros et al., 1994a; Mason et al., 1995).

Collagen Fiber Orientation

Using the diamond blade saw, a 1-mm-thick section was obtained from each of the PMMA-embedded segments that had been used for microstructure analyses. One surface was milled to a high luster finish (Reichert/Jung Ultramiller). The milled surface was then mounted with cyanoacrylate glue onto a slide, placed in moderate compression in a vice, and allowed to cure for 24 hr. The opposite side was then milled so that the embedded section had an overall uniform thickness of 100 (±5) μm.

According to the method of Boyde and Riggs (1990), milled sections were placed between appropriately crossed left- and right-hand sheets of circular polarizing material (HNCP37 × .030 inch filter; Polaroid Corporation, Norwood, MA) and analyzed for collagen fiber orientation with circularly polarized light (CPL). Sections were viewed in the light microscope, and regional differences in collagen fiber orientation are inferred from corresponding regional differences in the intensity of transmitted light, where darker gray levels represent relatively more longitudinal collagen and brighter gray levels represent relatively more oblique-to-transverse collagen. This method assumes that all other factors than can artifactually change the intensity of transmitted light (e.g., variations in specimen thickness) are eliminated.

By using algorithms of a commerically available image analysis system (Image 1, Universal Imaging Corporation, West Chester, PA) and a videocamera and monitor (Sony Video Camera Model DXC-750MD; Sony Trinitron Color Video Monitor Model PVM-1343MD, Japan), high-resolution black-and-white images (×62; approximately 2 mm^2) were captured directly from the microscope and stored onto disks. Gray-level values were subsequently quantified in the image taken in each cortical location where microstructural analysis had been done (Fig. 1). These imaged locations were immediately adjacent to the locations from which the ashed samples had been taken in the adjacent proximal segments. Uniformity of the light source (<0.5% variation) was verified in multiple locations before, intermittently during, and after image captures by using the algorithms of the imaging system.

Differences in transmitted light intensity were seen on the monitor as differences in gray levels (shades of gray). Image gray levels were converted into integer values ranging from 0, 1, 2, to 255. For each image, gray-level histograms were constructed after calculating the area fractions of pixels (as a fraction of total pixels) with a discrete gray level. By using the gray-level histograms, a weighted mean gray level (WMGL) was calculated according to the methods described by Boyce et al. (1990) and Skedros et al. (1993b). The darkest gray levels (0, 1, 2, . . . 25), were eliminated from the calculation of WMGLs because they represent porous spaces and other tissue voids. Average WMGLs were determined for each cortical region and sector.

Correlations With Strain Data

Values of normal strain, shear strain, peak strain energy density (SED), and summed SED were obtained from finite element mesh data in the recent study by Gross et al. (1992; Fig. 2). These published data were obtained from the midshaft of the third metacarpal of a 460-kg, 5-year-old thoroughbred that had not been race training for at least 1 year prior to experimentation (T.S. Gross and C.T. Rubin, personal communication). The strain distributions published in their studies of thoroughbreds at submaximal speeds are virtually identical to those that have been measured using the same methods at the mid-diaphyses of standard-breed horse during similar gaits (C.T. Rubin, unpublished data, personal communication). This similarity justifies the use of the published data for the purposes of the comparisons described in the present study. In addition, an extensive radiological study of multiple breeds including thoroughbred and mixed breeds showed little variation in size, geometry, and cortical thickness of limb bones between animals of comparable size (Hanson and Markel, 1994). However, direct comparison of third metacarpal cross-sectional shape between thoroughbred and standard breed horses has not been done.

Martin and Burr (1989, p. 163) defined SED as the product of stress and strain. Gross et al. (1992) calculated SED by using normal and shear strains at each finite element in the cortex via the Clapeyron formula, which is a continuum mechanics formula for SED. Strain energy density has two characteristics that distinguishes it from both stress and strain: (1) it is a scalar rather than tensor, and (2) it is always positive regardless of whether the loads are tensile or compressive. These characteristics mean that SED is a simpler variable than strain, and therefore it may be a more tractable signal by a bone's mechanosensitive cell population (Martin and Burr, 1989). Peak SED refers to the maximum strain energy density measured during the gait cycle. Summed SED is the summation of SED data experienced during an entire stance phase of the gait cycle. These and the other strain features that are considered herein have been considered to be powerful correlates to bone adaptation (Brown et al., 1990; Gross et al., 1992; Mullender and Huiskes, 1995).

The two elements in the mesh that coincided with the imaged regions were averaged and used to compute least mean square linear regressions by comparing the

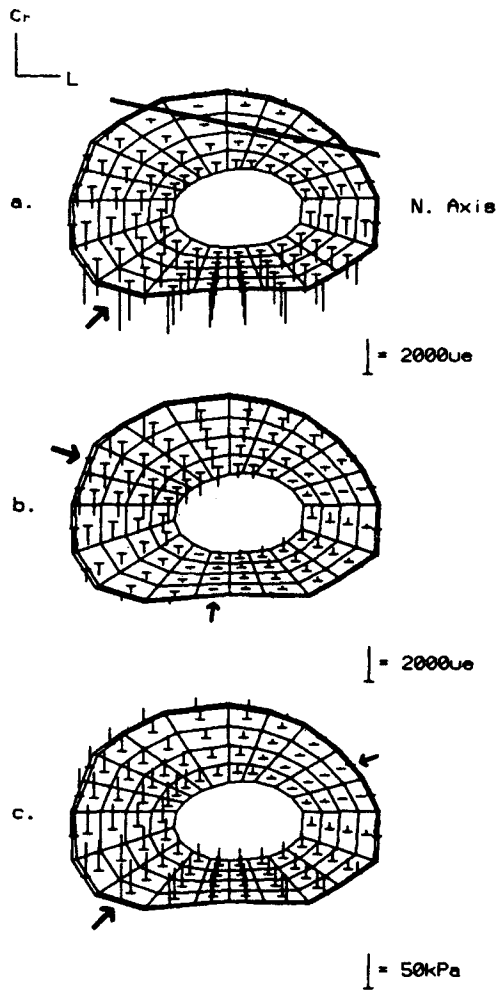

Fig. 2. Finite element meshes from Gross et al. (1992). Distribution of normal strain (a), shear strain (b), and SED (c) acting on the mid-shaft cross section at the time of peak strain during the gait cycle (sites of maximum strain are noted by the large arrows, sites of least strain by the small arrows). Peak shear strains (1,500 microstrain) were 63% of the magnitude of peak compressive strain (−2,400 microstrain), and SED varied by over two orders of magnitude across the cross section (max. = 54 kPa, min. = 0.1 kPa). The location of the neutral axis coincided with small shear strain magnitudes in the craniolateral cortex, resulting in a portion of this cortical area experiencing only minimal SED. (Reprinted from Journal of Biomechanics, Vol. 25, "Characterizing bone strain distributions in vivo using three triple rosette strain gages," pp. 1081–1087, with kind permission from Elsevier Science LTD, The Boulevard, Lanford Lane, Kidlington OX5 1GB, UK.)

structural and microstructural variables to normal strain, shear strain, peak SED, and summed SED. Values of normal strain were compared as respective positive (tension) and negative (compression) values and as absolute values.

Statistical Analysis

Nonnormally distributed parameters (porosity, collagen fiber orientation, mineral content, and cortical thickness) were analyzed by using the Kruskal-Wallis test, with Dunn's multiple comparisons post hoc testing for intergroup differences. The remaining parameters were normally distributed (OPD and FASB) and therefore were analyzed with a one-way analysis of variance (ANOVA) with Student Newman-Keuls post hoc testing for identifying intergroup differences. All possible pairwise comparisons were made between intracortical regions.

For ANOVA tests, data were grouped by region and by sector. Two-way ANOVA showed no interactions between region and sector for each of the variables in this study. Data were then further combined into two groups according to the predominant strain mode experienced in each region. A Student t test was used to compare normally distributed data and the Mann-Whitney test was used to compare nonnormally distributed data. Because the neutral axis of bending rotates laterally during portions of the gait cycle and with increasing gait speeds (Gross et al., 1991, 1992), portions of the lateral cortex receive intermittent tension and compression loads. Thus, four separate data groupings were analyzed according to sectors that, at times, experience prevailing tension strains vs. sectors experiencing prevailing compression strains: (1) cranial, craniolateral, and lateral vs. all other sectors, (2) cranial, craniolateral, and lateral vs. caudolateral, caudal, and caudomedial, (3) craniolateral and lateral vs. all other sectors, and (4) craniolateral and lateral vs. caudolateral, caudal, and caudomedial.

Comparisons with $P < 0.05$ were considered statistically significant. In addition, statistical trends ($0.05 < P < 0.1$) are also reported.

RESULTS

Inter- and Intraanimal Variations

The data were initially examined for variation that might be attributable to advanced age or some other factor (Martin and Burr, 1989; Stover et al., 1992). One animal was found to have markedly higher porosity (>2 SD above the mean in its caudal and cranial sectors) and relatively homogeneous mineral content and OPD between cortical sectors as compared with the other animals. This animal demonstrated the same pattern and magnitude of more oblique-to-transverse collagen in the caudal cortices and more longitudinal collagen in the craniolateral and lateral sectors than in the remaining animals. It is unclear whether this discrepancy is due to advanced age or to other factors. Therefore, this outlier was excluded from the sample, making the final sample size n = 9 for the results reported below.

Comparisons of Regions Within Each Sector (Table 1)

Microstructure

Representative BSE micrographs are shown in Figure 3. The middle region has a higher OPD than the endosteal region in each of the following sectors: cranial ($P = 0.005$), craniolateral ($P = 0.02$), caudolateral ($P = 0.03$), caudal ($P = 0.08$), caudomedial ($P = 0.06$), medial ($P = 0.006$), and craniomedial ($P = 0.02$). The periosteal region has a higher OPD than the endosteal region in each of the following sectors: cranial ($P = 0.07$), caudomedial ($P = 0.06$), and medial ($P = 0.01$). Similarly, FASB is greater in the periosteal region than in endosteal region in each of the following sectors: cranial ($P = 0.004$), caudolateral ($P = 0.001$), caudomedial ($P = 0.006$), medial ($P = 0.005$), and

TABLE 1. Means and standard deviations for individual regions[1]

Region	OPD (ost/mm^2)		FASB × 100 (%)		Porosity (%)		Gray level (wmgl)		Mineral (%)	
Sector	Mean	SD	Mean	SD	Mean	SD	Mean	SD	Mean	SD
Periosteal										
Cranial	16.4	6.9	42.6	15.9	5.2	1.8	161.9	23.7	69.6	2.7
Craniolateral	12.0	5.6	30.6	13.7	4.2	0.6	129.8	19.9	70.0	0.8
Lateral	13.8	5.8	41.2	18.7	4.3	1.2	123.7	24.9	69.3	1.6
Caudolateral	17.8	5.6	57.4	12.6	5.7	1.9	149.0	35.1	65.3	3.0
Caudal	18.1	5.8	51.0	10.6	6.4	3.8	182.0	22.1	66.7	1.7
Caudomedial	18.1	7.1	51.5	10.2	5.9	2.0	168.2	31.4	63.4	9.1
Medial	18.6	7.8	50.5	17.7	4.7	0.9	160.7	46.9	70.4	3.3
Craniomedial	13.5	8.9	42.7	25.3	4.7	1.3	161.5	40.0	70.8	3.7
Middle										
Cranial	20.3	6.4	47.8	14.0	4.9	1.3	148.4	32.9	69.6	0.7
Craniolateral	17.2	6.7	41.1	15.7	5.0	1.6	126.5	19.2	69.7	6.4
Lateral	16.0	6.5	41.2	19.0	3.8	1.0	109.5	18.6	70.8	2.9
Caudolateral	20.5	8.0	46.2	13.1	5.3	1.5	139.1	26.6	66.1	7.3
Caudal	19.6	9.1	45.7	15.6	5.9	3.6	164.3	36.9	67.7	6.3
Caudomedial	14.9	6.5	42.5	16.3	6.5	3.7	150.3	24.1	69.8	3.0
Medial	19.6	8.7	50.2	19.4	4.4	1.4	130.3	33.6	73.2	5.7
Craniomedial	19.3	9.2	46.4	16.7	4.7	1.5	128.6	32.0	70.6	3.0
Endosteal										
Cranial	10.7	6.5	21.7	11.3	5.6	3.5	134.5	11.1	68.4	12.3
Craniolateral	10.3	5.5	25.5	14.7	5.1	1.4	118.1	2.9	67.3	9.7
Lateral	12.6	4.2	32.4	14.7	4.5	1.2	109.8	9.9	71.2	4.0
Caudolateral	13.5	4.7	36.0	9.9	5.4	2.1	145.6	12.3	68.5	2.2
Caudal	13.7	4.8	36.6	9.3	5.1	2.4	166.9	18.6	67.9	7.2
Caudomedial	12.6	3.7	33.0	12.0	4.6	2.4	161.2	25.7	68.0	1.3
Medial	9.5	3.8	26.7	10.7	4.8	1.7	125.9	13.8	68.7	11.5
Craniomedial	10.9	3.6	25.1	11.6	4.5	1.4	117.5	17.3	70.4	8.8
ANOVA results	$P = 0.0001$		$P = 0.0001$		$*P < 0.0001$		$*P < 0.0001$		$*P < 0.0001$	

[1]OPD, osteon population density; FASB, fractional area of secondary bone. ANOVA results represent comparisons between the 24 individual regions.
*Kruskal-Wallis test used.

craniomedial ($P = 0.06$). FASB is greater in the middle region than in the endosteal region in each of the following sectors: cranial ($P = 0.005$), craniolateral ($P = 0.03$), caudolateral ($P = 0.08$), medial ($P = 0.006$), and craniomedial ($P = 0.06$). There are no significant differences in porosity between middle and periosteal regions at any of the sector locations. The endosteal region is more porous than the periosteal region in only the medial sector ($P = 0.03$).

Collagen fiber orientation

In the lateral sector, gray levels are brighter (more obliquely oriented collagen) in the periosteal region than in the middle ($P = 0.09$) and endosteal ($P = 0.04$) regions.

Comparisons Between Sectors (Table 2)

Cortical thickness

The caudal sector is 40% thinner than the cranial sector ($P < 0.01$), 40% thinner than the lateral sector ($P < 0.01$), 37% thinner than the craniolateral sector ($P < 0.01$), 50% thinner than the medial sector ($P < 0.001$), and 51% thinner than the craniomedial sector ($P < 0.001$). The caudomedial sector is 44% thinner than each of the medial and craniomedial sectors ($P < 0.01$). The caudolateral sector is 40% thinner than each of the medial and craniomedial sectors ($P < 0.001$).

Microstructure

The FASB in the craniolateral sector is 30% lower than in the caudolateral sector, 27% lower than in the caudal sector, and 24% lower than in the medial sector ($P < 0.05$). The cranial sector has 20% lower FASB than the caudolateral sector ($P = 0.05$). The lateral sector has 18% lower FASB than the caudolateral sector ($P = 0.07$). The craniomedial sector has 18% lower FASB than the caudolateral sector ($P = 0.07$; Fig. 4). The craniolateral sector has 24% lower OPD than each of the caudal and caudolateral sectors ($P < 0.05$). Porosity in the caudolateral sector is 15% greater than in the craniolateral sector, 30% greater than in the lateral sector, and 17% greater than in each of the medial and craniomedial sectors ($P < 0.05$).

Collagen fiber orientation

Representative circularly polarized images are shown in Figure 5. The lateral sector is 28% darker than the caudomedial ($P < 0.001$), 33% darker than the caudal sector ($P < 0.001$), and 21% darker than the caudolateral sector ($P < 0.05$). The craniolateral sector is 22% darker than the caudomedial sector ($P < 0.01$), 27% darker than the caudal sector ($P < 0.001$) and 16% darker than the cranial sector ($P < 0.05$). The medial and craniomedial sectors are, respectively, 19% and 21% darker than the caudal sector ($P < 0.05$; Fig. 6).

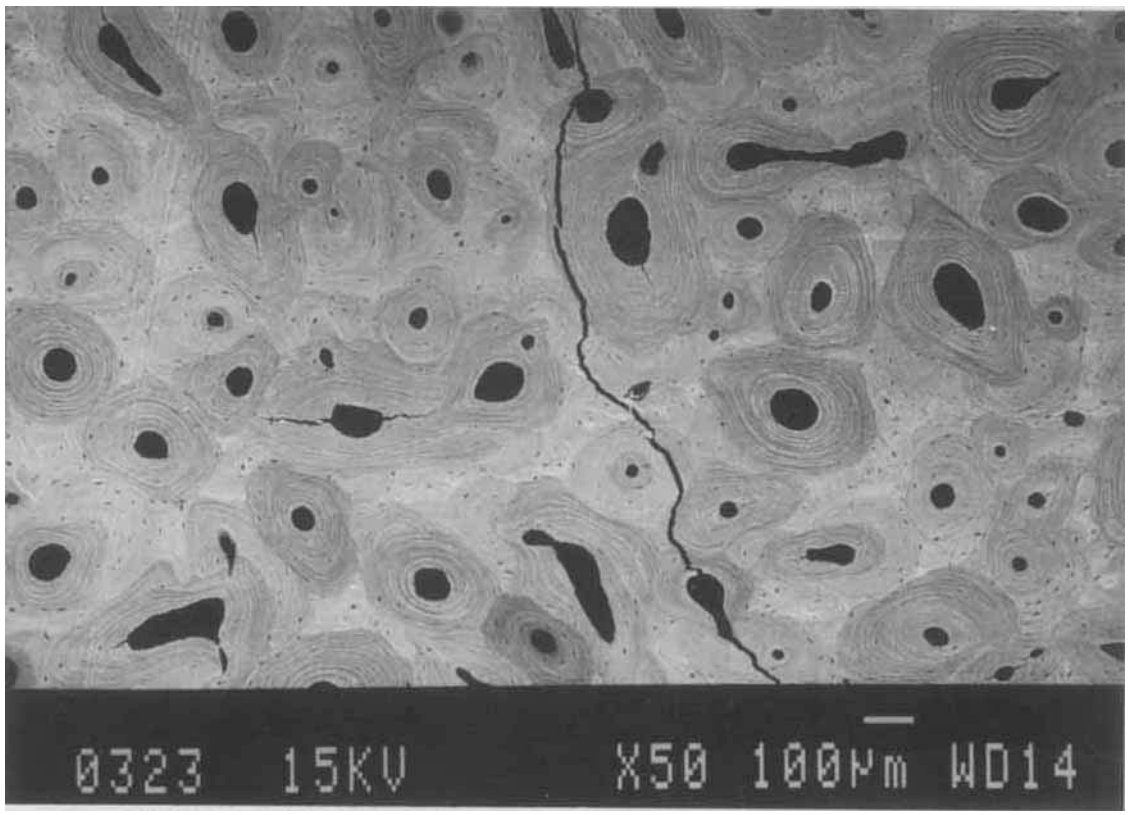

A. Middle region, craniolateral sector

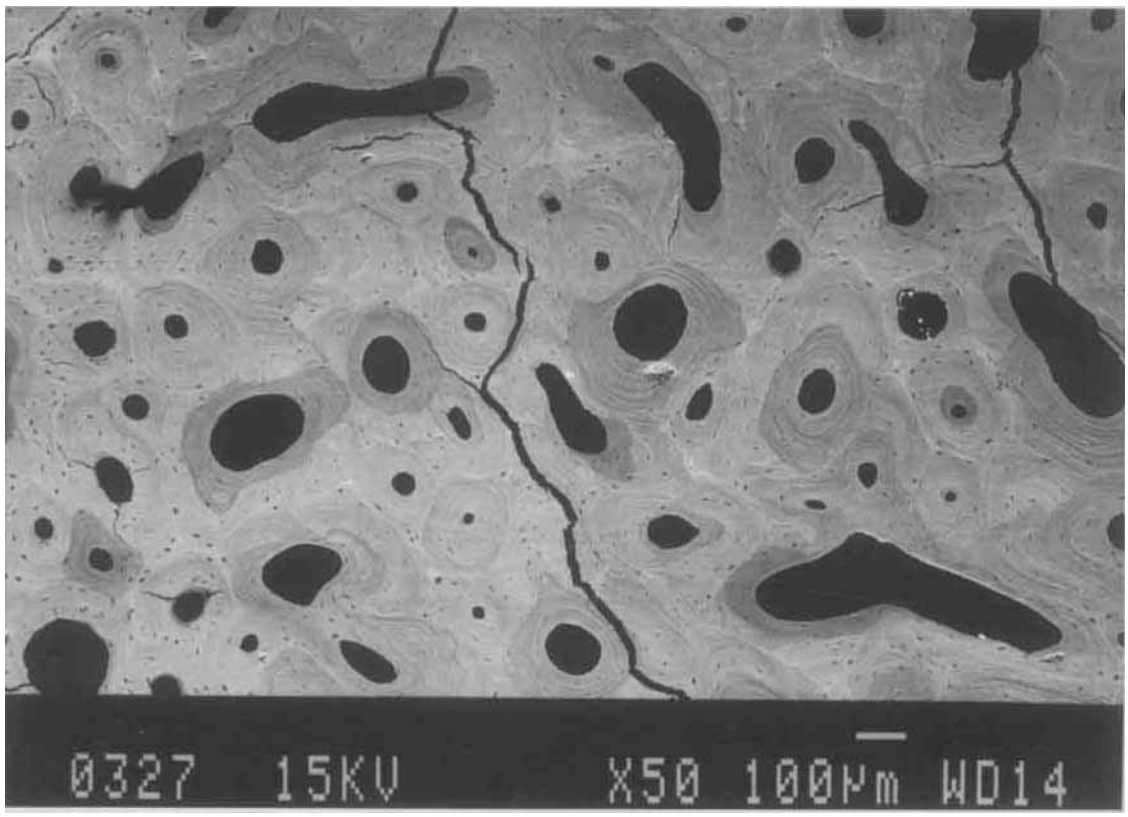

B. Middle region, caudomedial sector

Fig. 3. Backscattered electron images show representative microstructural differences between middle regions of craniolateral ("tension") (**A**) and caudomedial ("compression") (**B**) cortices of the same bone section.

TABLE 2. Sector comparisons: Means and standard deviations

	OPD (ost/mm^2)		FASB × 100 (%)		Porosity (%)		Gray level (wmgl)		Mineral (% ash)		Cortical thickness (mm)	
Sector	Mean	SD	Mean	SD	Mean	SD	Mean	SD	Mean	SD	Mean	SD
Cranial	15.8	7.5	37.4	17.6	5.2	2.3	148.3	25.6	69.2	7.0	9.7	1.6
Craniolateral	13.2	6.5	32.4	15.6	4.8	1.3	124.8	15.9	69.0	6.6	9.1	1.2
Lateral	14.1	5.6	38.2	17.4	4.2	1.1	114.3	19.0	70.4	3.0	9.4	1.1
Caudolateral	17.2	6.7	46.5	14.6	5.5	1.8	144.6	25.2	66.6	4.8	6.9	0.6
Caudal	17.1	7.0	44.4	13.2	5.8	3.2	171.1	26.6	67.4	5.4	5.7	0.6
Caudomedial	15.2	6.2	42.3	14.7	5.6	2.8	159.9	26.7	67.1	6.0	6.4	0.6
Medial	15.9	8.3	42.5	19.4	4.7	1.3	139.0	35.9	70.8	7.6	11.6	1.5
Craniomedial	14.6	8.2	38.1	20.3	4.6	1.3	135.9	35.1	70.6	5.6	11.6	1.5
ANOVA results[1]	$P = 0.0045$		$P = 0.0001$		*$P < 0.0001$		*$P < 0.0001$		*$P < 0.0001$		*$P < 0.0001$	

[1]The P values represent one-way ANOVA comparisons of data between sectors.
*Kruskal-Wallis test used. Two-way ANOVA using region (three levels) and sector (eight levels) as factors showed no interactions between region and sector for any variable ($P > 0.4$).

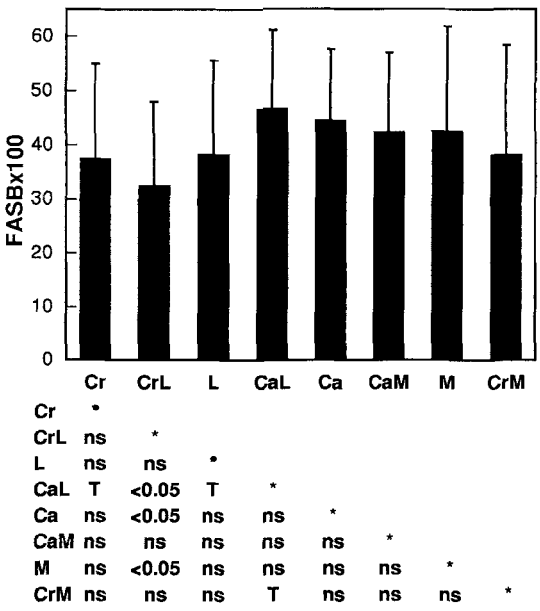

Fig. 4. Fractional area of secondary bone (FASB) at each sector location (n = 9 animals). Means and standard deviations (error bars) are shown. Statistically significant differences are shown in the matrix. T, trends approaching statistical significance ($0.05 < P < 0.1$); ns, nonsignificant ($P > 0.1$); Cr, cranial; CrL, craniolateral; L, lateral; CaL, caudolateral; Ca, caudal; CaM, caudomedial; M, medial; CrM, craniomedial.

Mineral content

The percentage of ash of the caudolateral sector is 3.7% less than in the cranial sector ($P < 0.05$), 3.4% less than in the craniolateral sector ($P < 0.001$), 5.4% less than in the lateral sector ($P < 0.01$), 5.6% less than in the medial sector ($P < 0.001$), and 5.6% less than in the craniomedial sector ($P < 0.001$). The percentage of ash in the caudal sector is 2.3% lower than in the craniolateral sector ($P < 0.05$) and 5.0% lower than in the medial sector ($P < 0.01$). The percentage of ash in the caudomedial sector is 2.8% lower than in the craniolateral sector ($P < 0.01$), 4.8% lower than in the lateral sector ($P < 0.05$), 5.2% lower than in the medial sector ($P < 0.001$), and 5.0% lower than in the craniomedial sector ($P < 0.001$).

Comparisons Between Tension and Compression Areas (Table 3)

Cranial, craniolateral, and lateral vs. all other sectors

FASB is 19% higher in the compression area ($P = 0.004$). For collagen fiber orientation, the compression area is 23% brighter ($P < 0.0001$). Several trends ($0.05 < P < 0.1$) that may be biologically significant were noted. OPD is 11% higher in the compression area ($P = 0.1$), and porosity is 11% greater in the compression area ($P = 0.1$). The percentage of ash is not statistically different between areas ($P = 0.3$).

Cranial, craniolateral, and lateral vs. caudolateral, caudal, and caudomedial

OPD is 15% higher in the compression area ($P = 0.04$). FASB is 8% higher in the compression area ($P = 0.0007$). Porosity is 19% higher in the compression area ($P = 0.04$). For collagen orientation, the compression area is 16% brighter ($P < 0.0001$). The percentage of ash is 3.5% lower in the compression area ($P = 0.005$).

Craniolateral and lateral vs. all other sectors

OPD is 17% higher in the compression area ($P = 0.05$). FASB is 19% higher in the compression area ($P = 0.01$). Porosity is 16% higher in the compression area ($P = 0.04$). For collagen orientation, the compression area is 25% brighter ($P < 0.0001$). The percentage of ash is 1.6% lower in the compression area ($P = 0.002$).

Craniolateral and lateral vs. caudolateral, caudal, and caudomedial

OPD is 21% higher in the compression area ($P = 0.01$). FASB is 26% higher in the compression area ($P = 0.0008$). Porosity is 24% higher in the compression area ($P = 0.01$). For collagen orientation, the compression area is 33% brighter ($P < 0.0001$). The percentage of ash is 3.9% lower in the compression area ($P = 0.004$).

Linear Correlations (Table 4)

The strongest correlations are observed when comparing gray level with normal strain ($r = 0.752$), gray level with shear strain ($r = 0.555$), gray level with summed SED ($r = 0.579$), cortical thickness with shear strain ($r = -0.614$) and cortical thickness with normal

strain ($r = 0.587$). The remainder of the correlation coefficients are low and reported in Table 4. Additional correlations in which all normal and shear strain magnitudes were converted to their absolute values are also reported in Table 4. For gray level (collagen fiber orientation), transformation of the normal and shear strains to their absolute values markedly decreases the correlation coefficients. In contrast, the magnitudes of the correlation coefficients remained essentially unchanged when the strain data are transformed for the other structural and material parameters. No discrete steps (that might indicate a threshold beyond which remodeling activity changes) were noted in any regression plots.

DISCUSSION

Many of the parameters measured in this study represent the microstructural manifestation of previous or current regional remodeling activities in the equine third metacarpal. Each secondary osteon fragment records an activation, resorption, and formation sequence and, hence, the history of remodeling activity in a given cortical location (Burr, 1992; Parfitt et al., 1996). Regional differences in cortical microstructure that have been observed, but often not quantified, in various bone types that are subject to habitual physiologic bending stresses have led many investigators to search for an association between remodeling and the prevailing strain environment (Amprino, 1943; Bacon and Griffiths, 1985; Biewener and Bertram, 1991; Biewener et al., 1986; Bouvier and Hylander, 1981; Boyde and Riggs, 1990; Bromage, 1992; Carando et al., 1989, 1991; Hert et al., 1994; Lanyon, 1984; Lanyon and Baggott, 1976; Lanyon and Bourn, 1979; Lanyon et al., 1979; Lozupone, 1985; McMahon et al., 1995; Portigliatti-Barbos et al., 1983; Reid and Boyde, 1987; Riggs et al., 1990, 1993a,b; Smith, 1960; Vincentelli, 1978). In recent quantitative studies, Riggs et al. (1993a,b) and Mason et al. (1995) reported lower FASB and OPD and more longitudinally oriented collagen fibers in the cranial (tension) cortex of skeletally mature horse radii than in the opposite (compression) cortex. Skedros et al. (1994b; Skedros, 1994; unpublished data) also found lower OPD and relatively more longitudinally oriented collagen fibers in the "tension" cortices of skeletally mature sheep radii, and deer, elk, sheep, and horse calcanei.

However, it is unclear if these and other documented microstructural differences reflect adaptation to prevailing strain mode or strain magnitude because the surface strains overlying the compression cortex are greater than those on the tension side (Martin and Burr, 1989). By using the finite element model of Gross et al. (1992), it is possible to examine more rigorously the equine third metacarpal for associations between mineral content, microstructural parameters and intracortical normal strain, shear strain, peak SED and summed SED.

The regression plots do not show discernible steps, thus diminishing, but not eliminating, the possibility that there are regional differences in bone material organization that are associated with threshold strain levels within this range of strain magnitudes. These data do not support the hypothesis that the magnitude of prevailing in vivo strain features, even over a wide range (up to $\times 30$ difference in compression magnitudes between the locations analyzed; Fig. 2), are correlated with the regional cortical material organization of this bone. Although these data do not show strong correlation of strain magnitudes with cortical bone material organization, they do not rule out the possibility that strain magnitudes may contribute a complex adaptive signal (Mason et al., 1995).

Linear correlations (Table 4) may indicate a functional relation between collagen fiber orientation and normal and shear strains. By convention, compression strains are negative numbers and tension strains are positive numbers (Martin and Burr, 1989). By converting strain values to their respective absolute values, the contribution of strain mode can be effectively eliminated. The marked decrease in correlation coefficients that is seen when collagen fiber orientation is compared with the absolute values of normal and shear strains suggests that strain mode may be a more important stimulus than strain magnitude for functional adaptive remodeling exhibited within the cortices of this bone.

The weak correlations shown between strains and other parameters measured in this study (Table 4) may have several explanations, including: (1) the given parameter is not influenced by or related to the intracortical strains that were examined in this study, (2) the successful maintenance of bone tissue requires strain information to be spatially integrated across the area of the cortex, implying that sites within a given cross section of the bone are "tuned" to vastly different levels of strain information (site specificity; Biewener and Bertram, 1993; Burr, 1992; Brand and Stanford, 1994); (3) the pertinent strain feature(s) or mechanical factor(s) that may be more strongly correlated with these differences was (were) not identified (e.g., strain rate, the strain tensor, fatigue life; Rubin et al., 1992; Burr, 1992; Kimmel, 1993; Turner et al., 1995); (4) the pertinent structural and material parameter(s) correlated with strain magnitude was not identiifed in this study (e.g., regional differences in lacunar-canalicular geometries, osteocyte population densities, or cell-matrix attachment protein densities; Weinbaum et al., 1994; Mullender and Huiskes, 1995; Brand and Stanford, 1994); (5) the stimulus (e.g., microcracks or even higher strain magnitudes than those present) for adaptation may be attenuated or ablated by the adaptive response and may no longer be present (Rubin and McLeod, 1990; Rubin et al., 1990); and (6) inadequate statistical power in the present study because of the sample size. In this list, number 2 is especially applicable to several of the "compression" locations because they receive markedly different strain magnitudes but share relatively similar cortical organizations. As suggested by Rubin et al. (1992), the fifth listed possibility is consistent with the idea that strain may not be causative but may simply be a consequence of the adaptive

Fig. 5. **A–D:** Circularly polarized light images show representative gray-level intensity (collagen fiber orientation) differences among the middle regions of cranial, caudal, medial, and lateral cortices of the same bone section. All images were obtained at the same illumination and magnification. The section is undecalcified, unstained, PMMA-embedded, and 100-μm thick. (Figure appears on the following pages.)

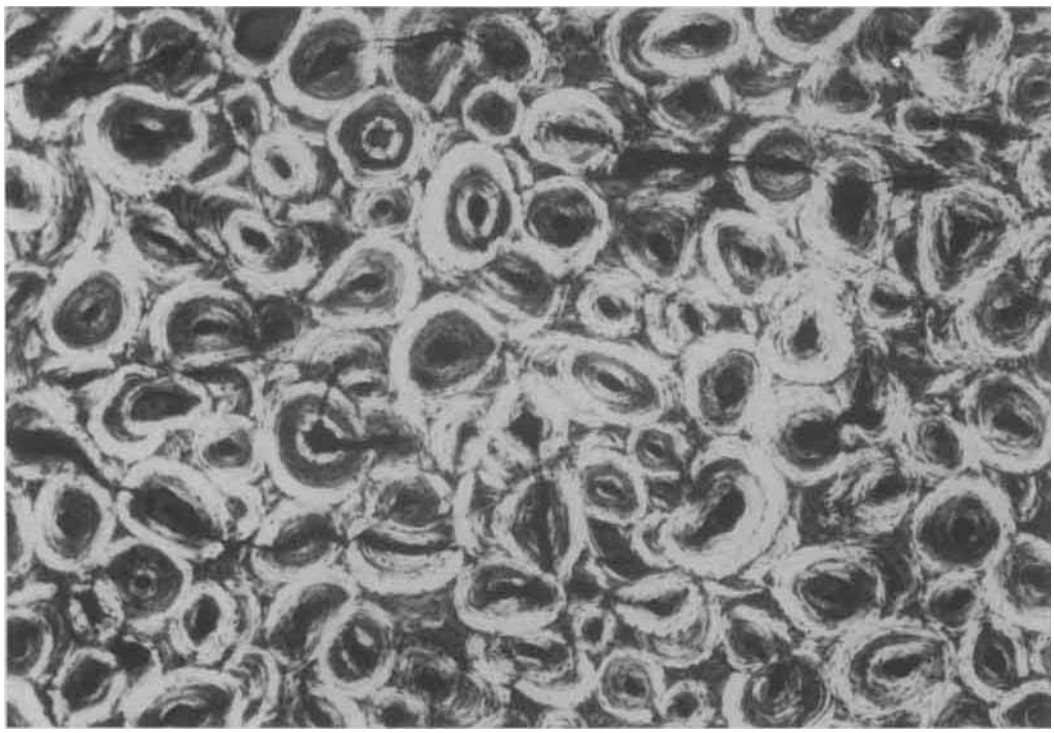

A. Middle region, cranial sector

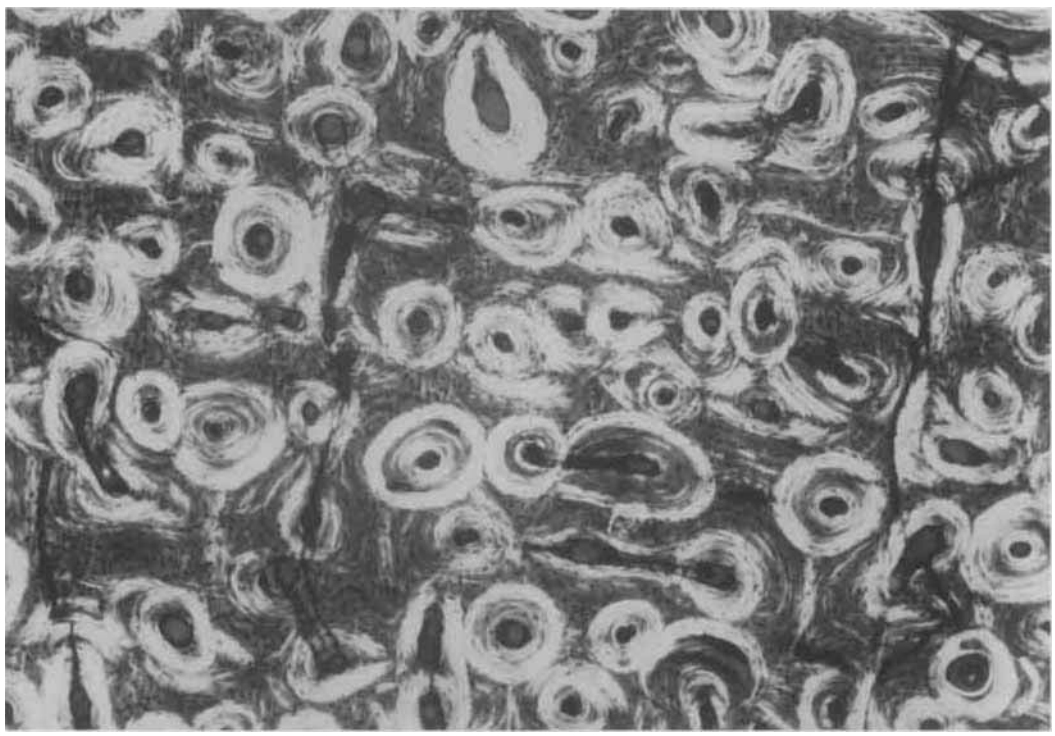

B. Middle region, medial sector

200 microns

Fig. 5a–b.

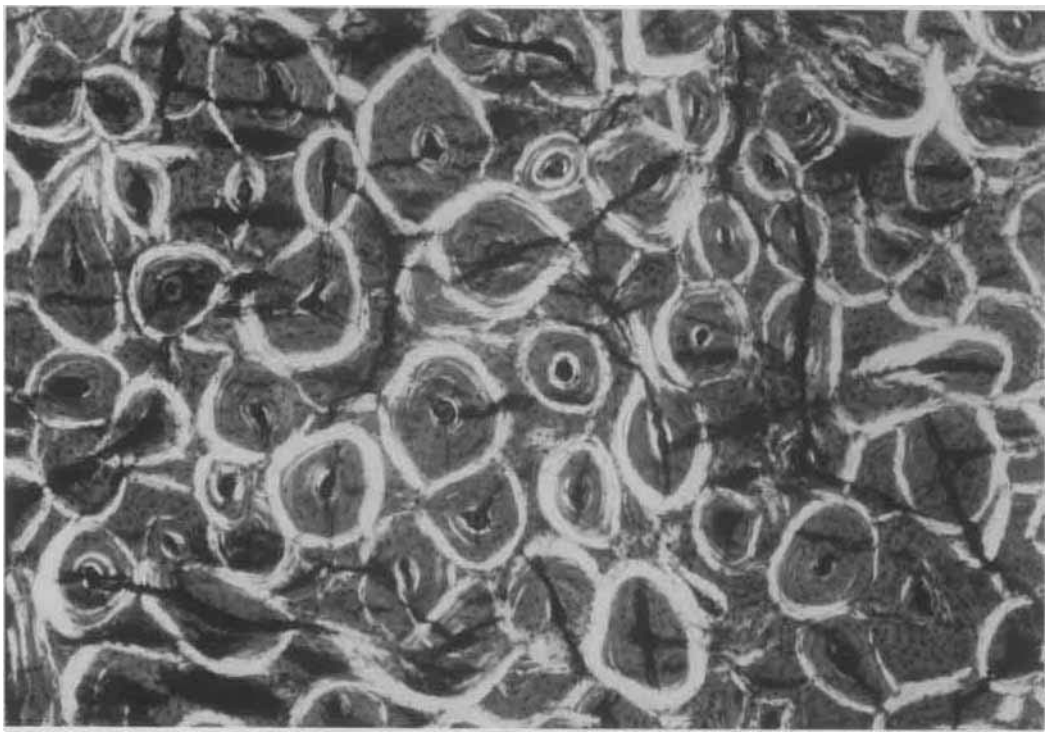

C. Middle region, lateral sector

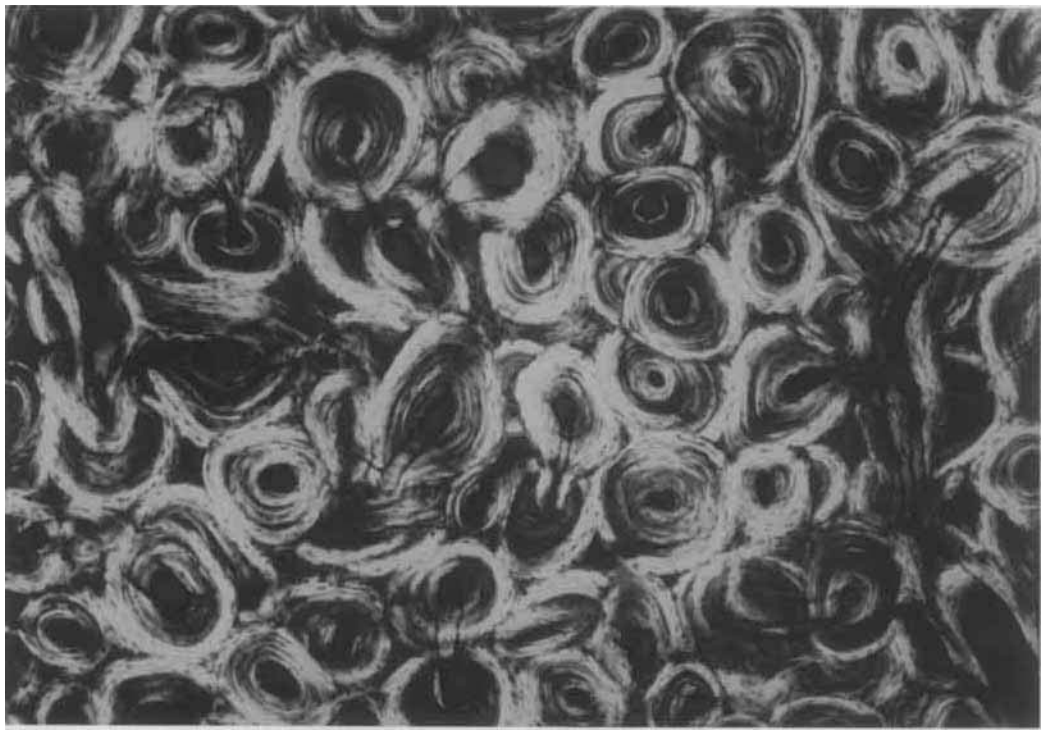

D. Middle region, caudal sector

200 microns

Fig. 5c–d.

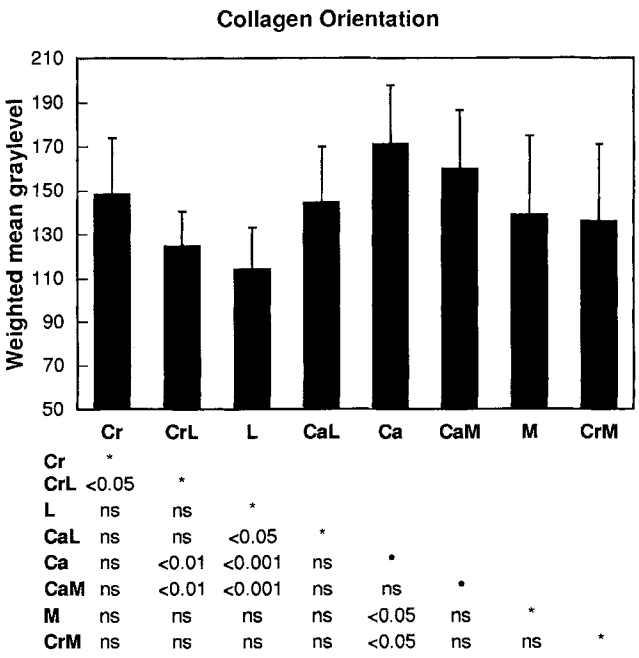

Fig. 6. Weighted mean gray-level (collagen fiber orientation) data at each sector location (n = 9 animals). Means and standard deviations (error bars) are shown. Statistically significant differences are shown in the matrix. Abbreviations are defined in Figure 4.

process. Although the issue of statistical power cannot be discounted, what does clearly emerge in the data is the apparent strain-mode-related adaptation of the collagen matrix. This finding has been consistently documented in various bones that experience habitual, directionally consistent, bending (Portagliatti-Barbos et al., 1983, 1984; Boyde and Riggs, 1990; Carando et al., 1989, 1991; Skedros, 1994).

The idea that strain mode has an important interdependent influence in compact bone adaptation seen in steady-state remodeling of skeletal maturity is discussed in our previous studies (Skedros, 1994; Skedros et al., 1994a,b; Mason et al., 1995). That strain mode may have influenced the structural and material organization of the equine third metacarpal is supported by (1) more longitudinal collagen in the craniolateral and lateral cortices and more oblique-to-transverse collagen in all other cortical sectors, (2) moderately strong correlation between collagen fiber orientation and normal and shear strains with poor correlation between collagen fiber orientation and the absolute values of normal and shear strains, and (3) significantly less FASB in the craniolateral cortex than all other sectors, lowest OPD in the craniolateral cortex, and significant differences in FASB between cortical sectors receiving tension and compression strains of similar magnitude. The possibility that similar regional differences in preferred collagen fiber orientation in compact bone are adaptations to tension vs. compression strain modes is also supported by previous experimental work that has documented strong correlations between mode-related mechanical properties and the preferred direction of bone lamellar collagen (Ascenzi, 1988; Simkin and Robin, 1974). Further support can be found in the studies of Riggs et al. (1993a,b) who showed that during growth of the equine radius the basic multicellular remodeling units (BMUs = forming secondary osteons) reorient collagen fibers in the compression cortex but not in the tension cortex. These differences could not be attributed to regional differences in the orientation of the secondary osteons.

Although the use of circularly polarized light to determine collagen fiber orientation in thin sections of bone has been pioneered by Portagliatti-Barbos, Boyde, and their co-workers (Portagliatti-Barbos et al., 1983, 1984; Boyde and Riggs, 1990), the idea that collagen fiber orientation reflects a long history of a customary strain-mode was originally championed by Gebhardt (1905). Research conducted during the 1930s and 1940s supported the hypothesis that the collagen matrix or OPD of long bones can exhibit apparent strain-mode-related adaptation. In a review of the European literature, Marotti (1963, p. 294) stated that "Bogdaschew (1936) found a different distribution of the osteons in the anterior and in the posterior-medial sector of the metacarpal shaft in horses of various races; also in this case a relationship occurs, in Bogdaschew's opinion, between bone structure and predominant type of stress" (Bogdaschew did not examine bone for collagen fiber orientation). Marotti stated further that [our notes are in brackets]:

> Godina (1946), however, did not record steady structural differences in the compacta of the metacarpus and of the femur in horses of various age [this was a qualitative study] . . . on the other had Olivo et al. (1937) observed clear-cut differences in the arrangement and structure of osteons [including collagen fiber orientation] in regions ["sectors" in the present study] of compacta [cow and mule principal metacarpals and metatarsals, and human femur] which presumably are subjected to stress of the opposite type. Structural differences were also described by Amprino (1943) [collagen fiber orientation was examined] in the cortex of the medial and lateral sectors of the upper part of the femoral diaphysis in man; under normal mechanical conditions these regions [sector locations] are subjected to qualitatively and quantitatively different stresses [or strain modes].

Although the finite element models of the mid-diaphysis of the equine third metacarpal do not show that tensile strains prevail across the entire breadth of the cranial, craniolateral, and lateral sectors (Fig. 2), the generally increased amount of longitudinal collagen in these sectors (Fig. 6) can be explained in this context if the strain milieu is examined at higher gait speeds. At high gait speeds, the neutral axis of the equine third metacarpal rotates laterally, which places the entire lateral cortex in tension (Gross et al., 1991; Gray and Rubin, 1988). Consequently, the increased thickness of the opposite medial and craniomedial sectors (Fig. 1) may be related to the higher compression strains that are sustained in these locations when this rotation occurs. Intermittent tension loading in the lateral cortex may explain the similarities of microstructure and collagen fiber orientation in the craniolateral (tension) and lateral (tension and compression) cortices. We hypothesize that these cortical areas exhibit increased longitudinal collagen fibers because they have experi-

TABLE 3. Tension and compression comparisons

Group[1]	OPD (ost/mm^2) Mean	SD	P[2]	FASB × 100 (%) Mean	SD	P	Porosity (%) Mean	SD	P	Gray level (wmgl) Mean	SD	P	Mineral (%) Mean	SD	P
1															
Tension	14.4	6.6		36.0	16.9		4.7	1.7		129.1	24.7		69.5	5.8	
Compression	16.0	7.3	0.1	42.8	16.7	0.004	5.2	2.2	0.1	150.1	32.5	0.0001	68.5	6.1	0.3
2															
Tension	14.4	6.6		36.0	16.9		4.7	1.7		129.1	24.7		69.5	5.8	
Compression	16.5	6.6	0.04	44.4	14.1	0.0007	5.6	2.6	0.04	158.5	27.9	0.0001	67.0	5.4	0.005
3															
Tension	13.6	6.0		35.3	16.6		4.5	1.2		119.6	18.0		69.7	5.1	
Compression	16.0	7.3	0.05	41.8	16.9	0.01	5.2	2.2	0.04	149.8	31.3	0.0001	68.6	6.3	0.002
4															
Tension	13.6	6.0		35.3	16.6		4.5	1.2		119.6	18.0		69.7	5.1	
Compression	16.5	6.6	0.01	44.4	14.1	0.0008	5.6	2.6	0.01	158.5	27.9	0.0001	67.0	5.4	0.004

[1]Group 1: cranial, craniolateral, and lateral versus all other sectors. Group 2: cranial, craniolateral, and lateral versus caudolateral, caudal, and caudomedial sectors. Group 3: craniolateral and lateral versus all other sectors. Group 4: craniolateral and lateral versus caudolateral, caudal, and caudomedial sectors.
[2]The P value represents comparison between the tension and compression areas in each group.

TABLE 4. Spearman correlation coefficients for comparisons between strain and observed data

	OPD r	P	FASB r	P	Porosity r	P	Gray level r	P	Mineral r	P	Thickness r	P
Normal	−0.180	0.009	−0.275	0.0001	−0.119	0.082	−0.752	0.0001	0.375	0.0001	0.587	0.0001
Shear	0.077	0.261	0.062	0.3630	0.010	0.885	−0.555	0.0001	−0.277	0.0001	−0.614	0.0001
Peak SED	0.172	0.012	0.284	0.0001	0.132	0.052	−0.444	0.0001	−0.281	0.0001	−0.279	0.0001
Summed SED	0.116	0.090	0.218	0.0010	0.091	0.185	0.579	0.0001	−0.108	0.115	0.007	0.919
Correlations with the absolute value of normal and shear strains												
Normal	0.17	0.012	0.273	0.0001	0.012	0.078	0.166	0.014	−0.375	0.0001	−0.585	0.0001
Shear	−0.166	0.015	−0.197	0.004	−0.096	0.159	−0.287	0.0001	0.379	0.0001	0.781	0.0001

enced a long history of a strain environment, where the amount of tension that they receive is "adequate" for evoking the matrix adaptations. The idea that the "amount" of tensile strain information that is required to evoke accommodative adaptation is much less than the "amount" of compressive strain information has been described as the "tension-resistance priority" hypothesis and is discussed by McMahon et al. (1995).

Riggs et al. (1993b) showed that collagen fiber orientation has a profound, if not preeminent, influence on elastic modulus at the midshaft of the horse radius. Their work strongly correlates longitudinal collagen in the cranial (tension) cortex with an increase in elastic modulus in tension loading and oblique-to-transverse collagen in the caudal (compression) cortex with a relative decrease in elastic modulus in compression loading. This finding is in contrast with the conventional view that collagen orientation differences such as these are adaptations that are aimed at resisting (not promoting) mode-related deformation (Evans, 1958; Simkin and Robin, 1974; Ascenzi, 1988; McMahon 1995). However, regional differences in collagen fiber orientation probably have less influence on elastic modulus in the horse third metacarpal because they are smaller than the magnitude of the difference reported in the radius. Extrapolating mechanical test data of Riggs et al. (1993b) in the horse radius to data reported in the present study suggests that the small regional differences in OPD and FASB measured in the horse third metacarpal would have, independent of altering collagen fiber orientation, little influence on altering regional elastic moduli. Mechanical testing of bone specimens from various locations for elastic and yield properties is currently being conducted to definitively evaluate all of these possibilities.

However, the possibility that during functional loading of the equine third metacarpal the regional differences in OPD, collagen fiber orientation, and mineral content might function in concert to enhance the mechanical competence of the bone material in the different cortical sectors is suggested by data reported by Stover et al. (1995) and Les et al. (1995). By examining compressive properties of cortical bone specimens obtained from various locations of the mid-diaphyses of equine third metacarpals, these investigators showed that the cranial cortex is significantly less ductile than the caudal cortex. Additional testing showed that fatigue life is greatest in the cranial cortex. The possibility that these regional differences represent biomechanically important material adaptations is supported by (1) data showing that differences in OPD can significantly alter the fatigue life and fracture toughness of bone material (Martin and Burr, 1989), and (2) the high incidence of two major disorders involving the cranial cortex in race horses: "bucked shins" and stress fractures, where the normal capacity to remodel bone cannot keep pace with the microdamage burden. These two maladies affect more than 70% of horses in race training (Norwood, 1978). Hence, re-

gional collagen fiber orientation and OPD differences reported in the present study may be aimed at accommodating the marked disparities in elastic, yield, and fatigue behavior of compact bone when loaded in tension vs. compression (Skedros et al., 1994a,b).

In quantitative studies Skedros et al. (1994b) and Mason et al. (1995) reported relatively lower OPD and FASB within the endosteal regions of the tension and compression cortices in deer calcanei and relatively higher porosities in the endosteal regions of the cranial (tension) and caudal (compression) cortices in horse radii. Although such differences may be responses to variations of strain magnitudes across the cortex in accordance with Frost's mechanostat theory (Skedros et al., 1994b), these microstructural variations may be more strongly influenced by local tissue effects of the medullary canal (Currey, 1984; Frost, 1990; Martin and Burr, 1989). In the equine third metacarpal, OPD and FASB do not differ significantly between the periosteal and middle regions, yet are markedly lower in the endosteal region at most sector locations (Table 1). The strain mileu reported by Gross et al. (1992), however, does not show a corresponding abrupt change in transcortical strain magnitudes at these locations. Absence of expected strain-magnitude-related transcortical variations in OPD and FASB in both cranial and caudal cortices have also been reported in transverse sections of the mid-diaphysis of the equine radius (Mason et al., 1995). Absence of transcortical porosity differences have also been reported in the compression cortex of deer calcanei (Skedros et al., 1994b). These inconsistent data suggest that proximity to the medullary canal, and not local transcortical variations in strain magnitude, may be more influential in affecting the microstructural differences typically seen between the endosteal region and the other two regions of long bones in the normal limb skeleton.

The three caudal sectors of the third metacarpal average 4% lower mineral content than the average of all other sectors. This average is similar to the decreased mineralization reported by Schryver (1978) in the caudal cortices of third metacarpals of skeletally immature 18-month-old Shetland ponies. The lower mineralization of the caudal sectors of mature bones might contribute to reduced elastic moduli in these locations (Currey, 1984; Skedros et al., 1994a). However, based on studies by Ashman et al. (1984) and Ashman and Rho (1988), the mineral content data reported in the present study would not be expected to confer elastic modulus differences greater than those measured by Schryver. Referring to the work of Schryver and Ashman and co-workers, Gross et al. (1992) stated that elastic modulus differences up to 20% (which is greater than what would be predicted to be attributable to variations in mineral content in the mature bones examined in the present study; Ashman and Rho, 1988) would not be of a magnitude sufficient to produce the observed range in the strain milieu in their finite element model of the skeletally mature thoroughbred third metacarpal. This result supports the use of a uniform elastic modulus used by Gross et al. (1991, 1992) in their finite element model.

Bone structural elements (e.g., curvature, cross-sectional shape, cortical thickness, etc.), inertial loading, and local muscle forces may function in concert to ensure a predictable distribution of strains during the majority of controlled in vivo loading sustained by a limb bone (Bertram and Biewener, 1988; Biewener, 1991; Mason et al., 1995; Riggs et al., 1993a,b). Recent investigators have hypothesized that in some limb bones regional differences in cortical thickness and cross-sectional geometry help to promote a predictable bending (loading) environment during controlled functional activities (Biewener, 1991; Bertram and Biewener, 1988; Rubin and McLeod, 1990). We suggest that the regional differences in bone matrix organization, including cortical collagen fiber orientation, mineral content, and porosity of the equine third metacarpal, also contribute synergistically with the relatively more important role of cortical thickness (narrower in the three caudal sectors) and the asymmetric cross-sectional geometry (Piotrowski et al., 1983) to produce its predictable bending in the craniolateral-to-caudomedial direction. The assurance of loading predictability coupled to a bending domain may be an important objective of limb bone morphology because the mechanosensitive apparatus in bone has been shown to be responsive to differences in bioelectric potentials that are produced by tension and compression strains (Martin and Burr, 1989; Bassett, 1968). The putative importance of tension and compression strains in contributing to the strain-related milieu to which cells may be tuned is also supported by the fact that 70% or more of the locomotion-induced longitudinal strains measured in the equine third metacarpal and in nearly all other limb bones that have been measured in vivo are caused by bending (Martin and Burr, 1989; Biewener, 1991, 1993). If this interpretation is correct, the customary occurrence of dichotomous strain modes in a predictable distribution may be an important component of a signal that provides a cytologically beneficial stimulus to which bone cells are tuned for the maintenance of mechanically competent tissue, even though compact bone exhibits an inherent biomechanically significant disparity in various mechanical properties when loaded in tension vs. compression (Rubin et al., 1992; Rubin and McLeod, 1990; Skedros et al., 1994a,b; Mason et al., 1995).

Alternatively, regionally heterogeneous matrix organization within the same bone cross section may reflect cell–matrix interactions that are aimed at ensuring the production of a consistent strain distribution (Burr, 1992) or some parameter that the cells can recognize during functional loading. Although it is not yet clear whether bone cells perceive and respond to strain signals directly through mechanical perturbations of the cell or matrix or indirectly through byproducts of deformation such as stress-generated potentials, the idea that bone matrix construction may be important in producing a specific strain milieu during functional loading is supported by experimental evidence suggesting that the information that governs cell activity is mediated through the bone matrix (Burr, 1992; Lanyon, 1993; Brand and Stanford, 1994; Mullender and Huiskes, 1995). For these reasons, further studies are needed to determine the roles that regional differences in matrix structural, microstructural, and material organization may have in altering a bone's mechanical properties and functionally induced strain environment while promoting a cytologically beneficial

strain milieu and ensuring regional and whole bone mechanical competence.

The strain milieu examined in the present study was obtained from animals during controlled gaits. Therefore, this analysis is reticent to the myriad of time-varying strain patterns and magnitudes that would occur during various other motions such as abrupt stops and turns, bolts, and leaps. These motions could produce high strains of short duration that may be important signals for bone adaptation or maintenance (Skerry and Lanyon, 1995; Biewener and Bertram, 1993; Lanyon, 1987). Because some variations in microscopic organization of bone tissue within one bone may simply be related to regional differences in growth rates (Enlow, 1966; Ricqles et al., 1991), caution should be exercised when interpreting bone organization solely in the context of mechanical adaptation. However, the conspicuous differences between regional patterns of collagen fiber orientation, their consistent relation with the distribution of bending strains across the mid-diaphysis of the equine third metacarpal, and the similarly coupled patterns in the equine radius and in other "tension/compression" bones suggest that the recognition of the strain mode component of the internal mechanical strain milieu is an important variant factor (Rubin et al., 1990; Skedros, 1994) in influencing the matrix organization of these bones.

ACKNOWLEDGMENTS

This work was supported in part by the Department of Veterans Affairs Medical Research Funds, Salt Lake City, Utah. We thank Doug Ota, Cathy Sanderson, Gwenevere Shaw, Peter Dirksmeier, and Melvin Kuhni for their technical assistance, Todd M. Boyce of the Bone and Joint Center of Henry Ford Hospital, Detroit, Michigan, for his helpful comments, and Pat Campbell and Harlan Amstutz of the Joint Replacement Institute of Orthopaedic Hospital, Los Angeles, California, for the use of their laboratory facilities.

LITERATURE CITED

Amprino, R. 1943 La struttura delle ossa dell'uomo in relazione a turbe dell'accrescimento. Ricerche sufli scheletri di un gigante e di un nano. Arch. Ital. Anat. Embriol. *XLIX*:160–193.

Ascenzi, A. 1988 The micromechanics versus the macromechanics of cortical bone—A comprehensive presentation. J. Biomech. Eng., *110*:357–363.

Ashman, R.B., and J.H. Rho 1988 Elastic modulus of trabecular bone material. J. Biomech., *21*:177–181.

Ashman, R.B., S.C. Cowin, W.C. Van Buskirk, and J.C. Rice 1984 A continuous wave technique for the measurement of the elastic properties of cortical bone. J. Biomech., *17*:349–361.

Bacon, G.E., and R.K. Griffiths 1985 Texture, stress and age in the human femur. J. Anat., *143*:97–101.

Barth, R.W., J.L. Williams, and F.S. Kaplan 1992 Osteon morphometry in females with femoral neck fractures. Clin. Orthop., *283*: 178–186.

Bassett, C.A.L. 1968 Biologic significance of piezoelectricity. Calcif. Tissue Res., *1*:252–272.

Bertram, J.E.A., and A.A. Biewener 1988 Bone curvature: Sacrificing strength for load predictability? J. Theor. Biol., *131*:75–92.

Biewener, A.A. 1993 Safety factors in bone strength. Calcif. Tissue Int., *53(Suppl. 1)*:S68–S74.

Biewener, A.A. 1991 Musculoskeletal design in relation to body size. J. Biomech., *24*:19–29.

Biewener, A.A., and J.E.A. Bertram 1991 Bone growth modeling in relation to functional strain. Trans. Orthop. Res. Soc., *16*:9.

Biewener, A.A., and J.E.A. Bertram 1993 Skeletal strain patterns in relation to exercise training during growth. J. Exp. Biol., *185*:51–69.

Biewener, A.A., J. Thomason, A. Goodship, and L.E. Lanyon 1983a Bone stress in the horse forelimb during locomotion at different gaits: A comparison of two experimental methods. J. Biomech., *16*:565–576.

Biewener, A.A., J. Thomason, and L.E. Lanyon 1983b Mechanics of locomotion and jumping in the forelimb of the horse (*Equus*): In vivo stress developed in the radius and metacarpus. J. Zool. Lond., *201*:67–82.

Biewener, A.A., S.M. Swartz, and J.E.A. Bertram 1986 Bone modeling during growth: Dynamic strain equilibrium in the chick tibiotarsus. Calcif. Tissue Int., *39*:390–395.

Bloebaum, R.D., K.N. Bachus, and T.M. Boyce 1990 Backscattered electron imaging: The role in calcified tissue and implant analysis. J. Biomater. Appl., *5*:56–85.

Bogdaschew, Von N. 1930 Der Zusammenhang der anatomischen formen der metacarpal- und metatarsalknochen der haustiere mit dem histologischen bau und der chemisch-physikalischen eigenschaftern derselben. Anat. Anz. (Jena), *70*:113–154.

Bouvier, M., and W.L. Hylander 1981 Effect of bone strain on cortical bone structure in macaques (*Macaca mulatta*). J. Morphol., *167*: 1–12.

Boyce, T.M., R.D. Bloebaum, K.N. Bachus, and J.G. Skedros 1990 Reproducible method for calibrating the backscattered electron signal for quantitative assessment of mineral content in bone. Scan. Microsc., *4*:591–603.

Boyde, A., and C.M. Riggs 1990 The quantitative study of the orientation of collagen in compact bone slices. Bone, *11*:35–39.

Brand, R.A., and C.M. Stanford 1994 How connective tissues temporally process mechanical stimuli. Med. Hypotheses, *42*:99–104.

Bromage, T.G. 1992 Microstructural organization and biomechanics of Macaque circumorbital region, in: Structure, Function and Evolution of Teeth. P. Smith and E. Tchernov, eds. Freund Publishing House, London, pp. 257–272.

Brown, T.D., D.R. Pedersen, M.L. Gray, R.A. Brand, and C.T. Rubin 1990 Toward an identification of mechanical parameters initiating periosteal remodeling: A combined experimental and analytic approach. J. Biomech., *23*:893–905.

Burr, D.B. 1992 Orthopedic principles of skeletal growth, modeling and remodeling. In: Bone Biodynamics in Orthodontic and Orthopedic Treatment, Vol. 27. D.S. Carlson and S.A. Goldstein, eds. University of Michigan, Ann Arbor, pp. 15–50.

Carando, S., M.P. Barbos, A. Ascenzi, and A. Boyde 1989 Orientation of collagen in human tibial and fibular shaft and possible correlation with mechanical properties. Bone, *10*:139–142.

Carando, S., M. Portigliatti Barbos, A. Ascenzi, and A. Boyde 1991 Macroscopic shape of, and lamellar distribution within, the upper limb shafts, allowing inferences about mechanical properties. Bone, *12*:265–269.

Corondan, G., and W.L. Haworth 1986 A fractographic study of human long bone. J. Biomech., *19*:207–218.

Cowin, S.C. 1987 Bone remodeling of diaphyseal surfaces by torsional loads: Theoretical predictions. J. Biomech., *20*:1111–1120.

Currey, J.D. 1984 The Mechanical Adaptations of Bones. Princeton University Press, Princeton.

Davies, H.M.S., R.N. McCarthy, and L.B. Jeffcott 1993 Surface strain on the dorsal metacarpus of thoroughbreds at different speeds and gaits. Acta Anat., *146*:148–153.

Emmanual, J., C. Hornbeck, and R.D. Bloebaum 1987 A polymethyl methacrylate method for large specimens of mineralized bone with implants. Stain Technol., *62*:401–410.

Enlow, D.H. 1966 An evaluation of the use of bone histology in forensic medicine and anthropology. In: Studies on the Anatomy and Function of Bone and Joints. F.G. Evans, ed., Springer, New York, pp. 93–112.

Evans, F.G. 1958 Relations between the microstructure and tensile strength of human bone. Acta Anta., *35*:285–301.

Fretz, P.B., Cymbaluk, N.F., and J.W. Pharr 1984 Quantitative analysis of long-bone growth in the horse. Am. J. Vet. Res., *45*:1602–1609.

Frost, H.M. 1990 Skeletal structural adaptations to mechanical usage (SATMU): 2. Redefining Wolff's law: The remodeling problem. Anat. Rec., *226*:414–422.

Gebhardt, W. 1905 Uber funktionell wichtige anordnungsweisen der feineren und groberen bauelement des wirbeltierknochens. Roux Arch. Entwickl Org., *20*:187–322.

Godina, G. 1946 Trasformazioni strutturali della compatta delle ossa lunghe degli equidi durante l'accrescimento e nella senescenza. Arch. Ital. Anat. Embriol., *51*:219–241.

Gray, M.L., and C.T. Rubin 1988 The mechanical environment of the appendicular skeleton as determined by three rosette strain

gauges: Potential for a more complete strain calculation. Trans. Orthop. Res. Soc., *13*:240.
Gross, T.S., K.J. McLeod, and C.T. Rubin 1990 The skeletal consequences of extreme physical activity: The comparative strain milieu generated by treadmill and field conditions. Trans. Orthop. Res. Soc., *15*:108.
Gross, T.S., K.J. McLeod, and C.T. Rubin 1991 Strain energy density as a function of time: Characterizing the skeleton's functional strain history. Trans. Orthop. Res. Soc., *16*:420.
Gross, T.S., K.J. McLeod, and C.T. Rubin 1992 Characterizing bone strain distributions in vivo using three triple rosette strain gages. J. Biomech., *25*:1081–1087.
Hanson, P.D., and M.D. Markel 1994 Radiographic geometric variation of equine long bones. Am. J. Vet. Res., *55*:1220–1227.
Hert, J., P. Fiala, and M. Petrtyl 1994 Osteon orientation of the diaphysis of the long bones in man. Bone, *15*:269–277.
Kimmel, D.B. 1993 A paradigm for skeletal strength homeostasis. J. Bone Miner. Res., *8*:S515–S522.
Kimmel, D.B., and W.S.S. Jee 1983 Measurements of area, perimeter, and distance: Details of data collection in bone histomorphometry. In: Bone Histomorphometry: Techniques and Interpretation. R.R. Recker, ed. CRC Press, Boca Raton, pp. 90–108.
Lanyon, L.E. 1984 Functional strain as a determinant for bone remodeling. Calcif. Tissue Int., *36*:S56–S61.
Lanyon, L.E. 1987 Functional strain in bone tissue as an objective, and controlling stimulus for adaptive bone remodeling. J. Biomech., *20*:1083–1093.
Lanyon, L.E. 1993 Osteocytes, strain detection, bone modeling and remodeling. Calcif. Tissue Int., *53*:S102–S107.
Lanyon, L.E., and D.C. Baggott 1976 Mechanical function as an influence on the structure and form of bone. J. Bone Joint Surg., *58-B*:436–443.
Lanyon, L.E., and S. Bourn 1979 The influence of mechanical function on the development and remodeling of the tibia: An experimental study in sheep. J. Bone Joint Surg., *61-A*:263–273.
Lanyon, L.E., P.T. Magee, and D.G. Baggott 1979 The relationship of functional stress and strain to the processes of bone remodelling: An experimental study on the sheep radius. J. Biomech., *12*:593–600.
Les, C.M., Stover, S.M., Keyak, J.H., Taylor, K.T., and A.J. Kaneps 1995 Stiff and strong material properties are associated with brittle post-yield behavior in cortical bone. Trans. Orthop. Res. Soc., *20*:131.
Lozupone, E. 1985 The structure of the trabeculae of cancellous bone, 1. The calcaneus. Anat. Anz. (Jena), *159*:211–229.
McMahon, J.M., A. Boyde, and T.B. Bromage 1995 Pattern of collagen fiber orientation in the ovine calcaneal shaft and its relation to locomotor-induced stain. Anat. Rec., *242*:147–158.
Marotti, G. 1963 Quantitative studies on bone reconstruction, 1. The reconstruction in homotypic shaft bones. Acta Anat., *52*:291–333.
Martin, R.B., and D.B. Burr 1989 Structure, Function and Adaptation of Compact Bone. Raven Press, New York.
Mason, M.W., J.G. Skedros, and R.D. Bloebaum 1995 Evidence of strain-mode-related cortical adaptation in the diaphysis of the horse radius. Bone, *17*:229–237.
Mullender, M.G., and R. Huiskes 1995 Proposal for the regulatory mechanism of Wolff's law. J. Orthop. Res., *13*:503–512.
Norwood, G.L. 1978 The bucked-shin complex in thoroughbreds. Proc. Am. Assoc. Equine Pract., *24*:319–336; adaptation in the diaphysis of the horse radius. Bone, *17*:229–237.
Nunamaker, D.M., D.M. Butterweck, and M.T. Provost 1990 Fatigue fractures in thoroughbred racehorses: relationships with age, peak bone strain, and training. J. Orthop. Res., *8*:604–611.
Olivo, O.M., G. Maj, and E. Toaiari 1937 Sul significato della minuta struttura del tessuto osseo compatto. Boll. Sci. Med. (Bologna), *109*:369–394.
Palmer, S.E. 1986 Prevalence of carpal fractures in thoroughbred and standardbred racehorses. J. Am. Vet. Med. Assoc., *188*:1171–1173.
Parfitt, A.M. 1983 Stereologic basis of bone histomorphometry: Theory of quantitative microscopy and reconstruction of the third dimension. In: Bone Histomorphometry: Techniques and Interpretation. R.R. Recker, ed. CRC Press, Boca Raton, pp. 53–88.
Parfitt, A.M., G.R. Mundy, G.D. Roodman, D.E. Hughes, and B.F. Boyce 1996 A new model for the regulation of bone resorption, with particular reference to the effects of bisphosphonates. J. Bone Miner. Res., *11*:150–159.
Piotrowski, G., M. Sullivan, and P.T. Colahan 1983 Geometric properties of equine metacarpi. J. Biomech., *16*:129–139.
Portigliatti-Barbos, M., P. Bianco, and A. Ascenzi 1983 Distribution of osteonic and interstitial components in the human femoral shaft with reference to structure, calcification and mechanical properties. Acta Anat., *115*:178–186.
Portigliatti-Barbos, M., P. Bianco, A. Ascenzi, and A. Boyde 1984 Collagen orientation in compact bone: II. Distribution of lamellae in the whole of the human femoral shaft with reference to its mechanical properties. Metab. Bone Dis. Rel. Res., *5*:309–315.
Reid, S.A., and A. Boyde 1987 Changes in the mineral density distribution in human bone with age: Image analysis using backscattered electrons in the SEM. J. Bone Miner. Res., *2*:13–22.
Ricqles, A., F.J. Meunier, J. Castanet, and H. Francillon-Vieillot 1991 Comparative microstructure of bone. In: Bone Matrix and Bone Specific Products, Vol. 3. B.K. Hall, ed. CRC Press, Boca Raton, pp. 1–78.
Riggs, C.M., L.E. Lanyon, and A. Boyde 1990 Preferred orientation of the ultrastructural elements of bone: Relationship with strain. Trans. Orthop. Res. Soc., *15*:73.
Riggs, C.M., L.E. Lanyon, and A. Boyde 1993a Functional associations between collagen fibre orientation and locomotor strain direction in cortical bone of the equine radius. Anat. Embryol., *187*:231–238.
Riggs, C.M., L.C. Vaughan, G.P. Evans, L.E. Lanyon, and A. Boyde 1993b Mechanical implications of collagen fibre orientation in cortical bone of the equine radius. Anat. Embryol., *187*:239–248.
Rubin, C.T., and L.E. Lanyon 1982 Limb mechanics as a function of speed and gait: A study of functional strains in the radius and tibia of horse and dog. J. Exp. Biol., *101*:187–211.
Rubin, C.T., and K.J. McLeod 1990 Biologic modulation of mechanical influences in bone remodeling. In: Biomechanics of Diarthrodial Joints, vol. 2. V.C. Mow, A. Ratcliffe, and S.L.-Y. Woo, eds. Springer-Verlag, New York, pp 97–118.
Rubin, C.T., K.J. McLeod, and S.D. Bain 1990 Functional strains and cortical bone adaptation: Epigenetic assurance of skeletal integrity. J. Biomech., *23*:43–54.
Rubin, C.T., K.J. McLeod, T.S. Gross, and H.J. Donahue 1992 Physical stimuli as potent determinants of bone morphology. In: Bone Biodynamics in Orthodontic and Orthopedic Treatment, vol. 27. D.S. Carlson, and S.A. Goldstein, eds. University of Michigan, Ann Arbor, pp. 75–91.
Russ, J.C. 1986 Practical Stereology. Plenum Press, New York.
Schneider, R.K., D.W. Milne, A.A. Gabel, J.J. Groom, and L.R. Bramlage 1982 Multidirectional in vivo strain analysis of the equine radius and tibia during dynamic loading with and without a cast. Am. J. Vet. Res., *43*:1541–1550.
Schryver, H.F. 1978 Bending properties of cortical bone of the horse. Am. J. Vet. Res., *39*:25–28.
Simkin, A., and G. Robin 1974 Fracture formation in differing collagen fiber pattern of compact bone. J. Biomech., *7*:183–188.
Skedros, J.G. 1994 Collagen fiber orientation in skeletal tension/compression systems: A potential role of variant strain stimuli in the maintenance of cortical bone organization. J. Bone Miner. Res., *9*:B84.
Skedros, J.G., D. Ota, and R.D. Bloebaum 1993a Mineral content analysis of tension/compression skeletal systems: Indications of potential strain-specific differences. J. Bone Miner. Res., *8*:789.
Skedros, J.G., R.D. Bloebaum, K.N. Bachus, and T.M. Boyce 1993b The meaning of graylevels in backscattered electron images of bone. J. Biomed. Mater. Res., *27*:47–56.
Skedros, J.G., R.D. Bloebaum, K.N. Bachus, T.M. Boyce, and B. Constantz 1993c Influence of mineral content and composition on graylevels in backscattered electron images of bone. J. Biomed. Mater. Res., *27*:57–64.
Skedros, J.G., R.D. Bloebaum, M.W. Mason, and D.M. Bramble 1994a Analysis of a tension/compression skeletal system: Possible strain-specific differences in the hierarchial organization of bone. Anat. Rec., *239*:396–404.
Skedros, J.G., M.W. Mason, and R.D. Bloebaum 1994b Differences in osteonal micromorphologies between tensile and compressive cortices of a bending skeletal system: Indications of potential strain-specific differences in bone microstructure. Anat. Rec., *239*:405–413.
Skerry, T.M., and L.E. Lanyon 1995 Interruption of disuse by short duration walking exercise does not prevent bone loss in the sheep calcaneus. Bone, *16*:269–274.
Smith, J.W. 1960 The arrangement of collagen fibres in human secondary osteons. J. Bone Joint Surg., *42*:588–605.
Stover, S.M., R.R. Pool, R.B. Martin, and J.P. Morgan 1992 Histological features of the dorsal cortex of the third metacarpal bone mid-diaphysis during postnatal growth in thoroughbred horses. J. Anat., *181*:455–469.
Stover, S.M., R.B. Martin, V.A. Gibson, J.C. Gibeling, and L.V. Griffin

1995 Osteonal pullout increases fatigue life of cortical bone. Trans. Orthop. Res. Soc., *20:*129.

Turner, A.S., E.J. Mills, and A.A. Gabel 1975 In vivo measurement of bone strain in the horse. Am. J. Vet. Res., *36:*1573–1579.

Turner, C.H., I. Owan, Y. Takano 1995 Mechanotransduction in bone: Role of strain rate. Am. J. Physiol., *269(3):*E438–E442.

Vincentelli, R. 1978 Relation between collagen fiber orientation and age of osteon formation in human tibial cortical bone. Acta. Anat., *100:*120–128; Anat. Rec., *239:*405–413.

Weinbaum, S., S.C. Cowin, and Y. Zeng 1994 A model for the excitation of osteocytes by mechanical loading-induced bone fluid shear stresses. J. Biomech., *27:*339–360.